Extended Methods

Sigmoid Fitting

We used the following workflow to fit a sigmoid to the bar cross-sectional shapes (equation 1 in main text).

1. Finds X_0 as the central point on the interpolated bar surface
2. Finds L as channel depth set by the interpolation of channel bathymetry
3. Manually pick two points around X_0 such that $\frac{dy}{dx}$ best represents the bar slope, which sets $\frac{dy}{dx}$ at $f(x_0)$
4. When $X = X_0$, $\frac{d}{dx}\frac{L}{1+e^{k(x-x_0)}} = \frac{kL}{4}$, therefore $k = \frac{4}{L}\frac{dy}{dx}$

Bayesian Analysis

We use a Bayesian linear regression model to develop an empirical relationship between modern bar surface widths and bankfull channel widths. Bayesian linear regression assumes a probability distribution for the response variable, B_{bf}, and a prior distribution for relevant. We model:

$$B_{bf} = \alpha W_{bar} \qquad \text{(S1)}$$

with the aim to constrain a single parameter, α. To apply the Bayesian regression, we transformed the response and explanatory variables such that equation (S1) becomes:

$$log_{10}(B_{bf}) = log_{10}(\alpha) + log_{10}(W_{bar}) \qquad \text{(S2)}$$

The transformation is performed in order to assume that:

$$log_{10}(B_{bf,i})|\mu_i, \tau \sim \text{Normal}(\mu_i, \tau) \qquad \text{(S3)}$$

where μ_i is the mean for each transformed observation, and τ is a precision where $\tau \sim Uniform(0, 1000)$. We assume a prior distribution for α, $\alpha \sim Normal(0,\ 1000)$. Both the posterior probability distribution of the parameter mean and the posterior predictive distribution of predicted B_{bf} measurements are generated through Markov Chain Monte Carlo (MCMC) sampling done through the PyMC Python package and its NUTS sampler. We also modeled the data with two open parameters following the equation:

$$log(B_{bf}) = \log(\beta) + \gamma \log(W_{bar}) \qquad \text{(S4)}$$

More in-depth treatments of these methods can be found in Christensen et al. (2011) and Trampush et al. (2014).

Measuring Radius of Curvature

We computed the radius of curvature by fitting a least squares circle to centerline coordinates that fall within the active point bars. This produced a single estimate of radius of curvature at the bend scale (Fig. DR1). We followed method as outlined in the "Least squares circle" SciPy Cookbook at:
https://scipy-cookbook.readthedocs.io/items/Least_Squares_Circle.html

Estimating Channel Depths

While we had published channel depths for 9 out of 11 rivers, we had to estimate channel depths for the Koyukuk and Nestucca Rivers to perform the bathymetric interpolation. We applied the aspect-ratio scaling relationship from Ielpi and Lapôtre (2019) to estimate channel depth following:

$$h_{bf} = (0.17) \pm 0.05 B_{bf}{}^{(0.65 \pm 0.06)} \quad \text{(S5)}$$

We validated the aspect-ratio scaling on the rest of our data set, and each published depth value falls within the range of uncertainty given in S5 (Fig. DR2). We used mean model parameters to estimate the Koyukuk and Nestucca channel depths.

Code Availability

All code used in the analyses for this paper are openly available at:

https://github.com/evan-greenbrg/BarWidth

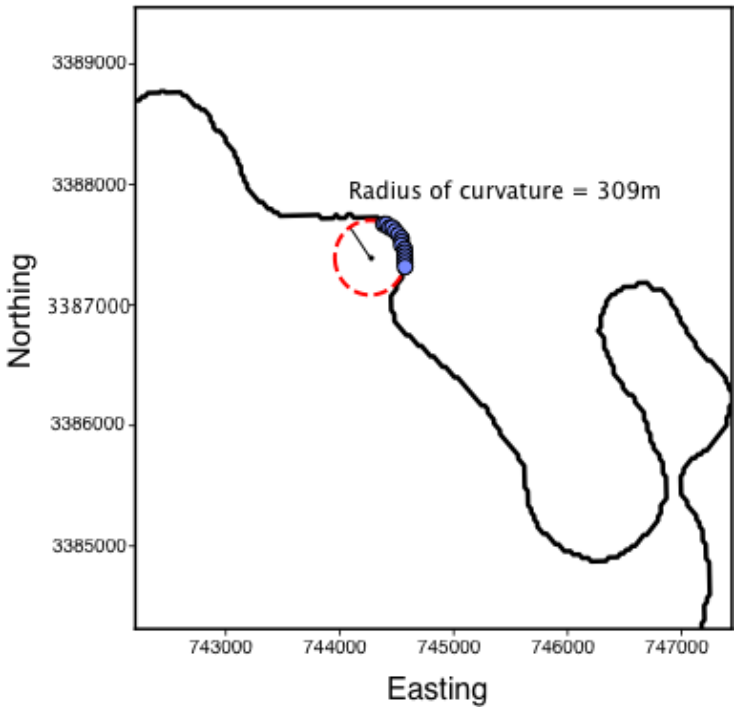

Figure DR1: Example radius of curvature estimation from the Brazos River. The black curve is the unsmoothed river centerline and blue points are sampled point bar coordinates. The reported radius of curvature is calculated from the fit red circle following the methods outlined above.

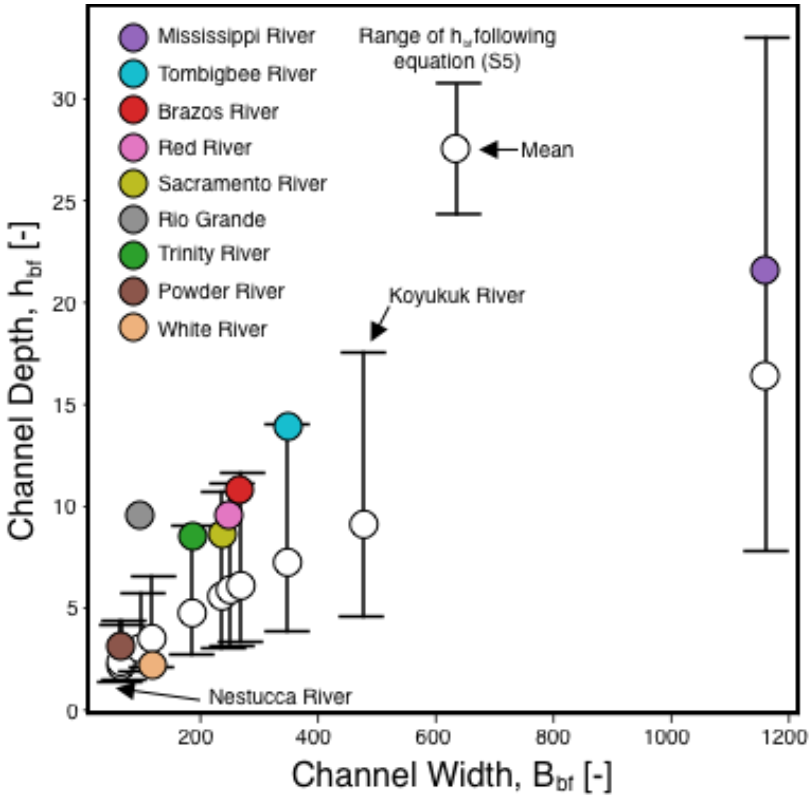

Figure DR2: Estimates of channel depth, h_{bf}, following equation (S5). Colored circles are the rivers with published values of depth. Error bars are the upper, lower and mean estimates following equation (S5). We use the mean (S5) estimate for h_{bf} of the Koyukuk and Nestucca rivers.

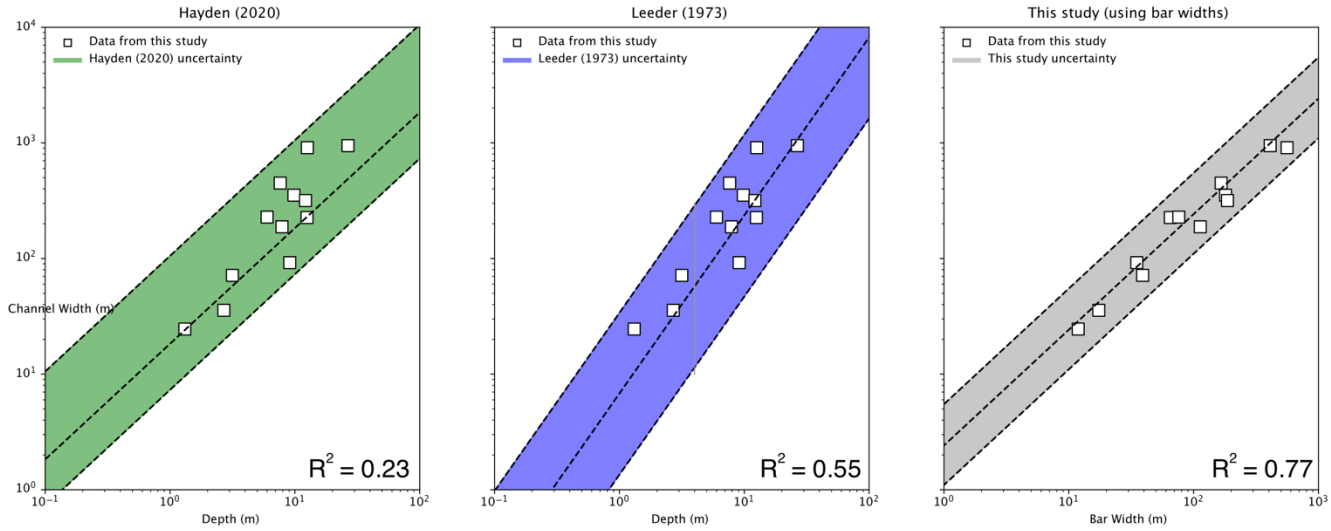

Figure DR3: Comparison between three methods to estimate B_{bf} from channel dimensions. The Hayden (2019) method uses a linear scaling between B_{bf} and h_{bf}, the Leeder (1973) method uses a power law scaling, and this study leverages the widths of bar clinoforms. White squares are the reach-averaged data reported in this study. R^2 values and model precision both improve with the application of bar clinoform widths over aspect-ratio scaling.

References Cited

Andreadis, K. M., Schumann, G. J.-P., and Pavelsky, T., 2013, A simple global river bankfull width and depth database: Water Resources Research, v. 49, p. 7164–7168. doi: https://doi.org/10.1002/wrcr.20440

Brice, J., 1977, Lateral Migration of the Middle Sacramento River, California; U.S. Geological Survey, Water-Resources Investigations 77-43, United States Department of the Interior, July, 1977.

Christensen, R., Johnson, W., Branscum, A., and Hanson, T. E., 2010, Bayesian Ideas and Data Analysis: An Introduction for Scientists and Statisticians (Chapman & Hall/CRC Texts in Statistical Science). CRC Press.

Donselaar, Marinus E., and Irina Overeem, 2008, Connectivity of Fluvial Point-Bar Deposits: An Example from the Miocene Huesca Fluvial Fan, Ebro Basin, Spain: AAPG Bulletin, v. 92, no. 9, p. 1109–29. doi:10.1306/04180807079.

Durkin, Paul R., Boyd, Ron L., Hubbard, Stephen M., Shultz, Albert W., Blum, Michael D., 2017, Three-Dimensional Reconstruction of Meander-Belt Evolution, Cretaceous Mcmurray Formation, Alberta Foreland Basin, Canada: Journal of Sedimentary Research, v. 87, no. 10, p. 1075–99. doi:10.2110/jsr.2017.59.

Ganti, V., Chu, Z., Lamb, M. P., Nittrouer, J. A., and Parker, G., 2014, Testing morphodynamic controls on the location and frequency of river avulsions on fans versus deltas: Huanghe (Yellow River), China: Geophysical Research Letters, v. 41, p. 7882–7890. doi: https://doi.org/10.1002/2014gl061918

Gautier, E., Brunstein, D., Vauchel, P., Jouanneau, J.-M., Roulet, M., Garcia, C., Guyot, J.-L., and Castro, M., 2010, Channel and floodplain sediment dynamics in a reach of the tropical meandering Rio Beni (Bolivian Amazonia): Earth Surface Processes and Landforms, v. 35, p. 1838–1853. doi: https://doi.org/10.1002/esp.2065

Hansford, M. R., Plink-Björklund, P., and Jones, E. R., 2020, Global quantitative analyses of river discharge variability and hydrograph shape with respect to climate types: Earth-Science Reviews, v. 200, 102977. doi: 10.1016/j.earscirev.2019.102977

Hayden, A. T., Lamb, M. P., Fischer, W. W., Ewing, R. C., McElroy, B. J., and Williams, R. M. E., 2019, Formation of sinuous ridges by inversion of river-channel belts in Utah, USA, with implications for Mars: Icarus, v. 332, p. 92–110. doi: 10.1016/j.icarus.2019.04.019.

Ielpi, A, 2018, Morphodynamics of meandering streams devoid of plant life: Amargosa River, Death Valley, California: GSA Bulletin, v. 131, p. 782–802. doi: https://doi.org/10.1130/b31960.1

Ielpi, A., and Ghinassi, M., 2014, Planform architecture, stratigraphic signature and morphodynamics of an exhumed Jurassic meander plain (Scalby Formation, Yorkshire, UK): Sedimentology, v. 61, p. 1923–1960. doi: 10.1111/sed.12122

Ielpi, A., and Lapôtre, M. G. A., 2019, A tenfold slowdown in river meander migration driven by plant life: Nature Geoscience, v. 13, p. 82–86. doi: 10.1038/s41561-019-0491-7.

Indiana Department of Natural Resources, Division of Fish & Wildlife, *White River Basin Survey: West Fork White River*, 2004, https://secure.in.gov/dnr/fishwild/files/fw-WFWR2004Basinreport.pdf

Kasvi, E., Vaaja, M., Kaartinen, H., Kukko, A., Jaakkola, A., Flener, C., Hyyppä, H., Hyyppä, J., and Alho, P., 2015, Sub-bend scale flow–sediment interaction of meander bends — A combined approach of field observations, close-range remote sensing and computational modelling: Geomorphology, v. 238, p. 119–134. doi: https://doi.org/10.1016/j.geomorph.2015.01.039

Leclair, S., 2011. Interpretingfluvial hydromorphology from the rock record: large-river peakflows leave no clear signature. In: Davidson, S.K., Leleu, S., North, C.P.(Eds.), From River to Rock Record: The Preservation of Fluvial Sediments andTheir Subsequent Interpretation, SEPM Special Publication No. 97, pp. 113–124.

Leeder, M. R., 1973, Fluviatile fining-upwards cycles and the magnitude of palaeochannels: Geological Magazine, v. 110, 265–276. doi: 10.1017/s0016756800036098

Lotsari, E., Vaaja, M., Flener, C., Kaartinen, H., Kukko, A., Kasvi, E., Hyyppä, H., Hyyppä, J., and Alho, P, 2014, Annual bank and point bar morphodynamics of a meandering river determined by high-accuracy multitemporal laser scanning and flow data: Water Resources Research, v. 50, p. 5532–5559. doi: https://doi.org/10.1002/2013wr014106

Moody, J. A., and Meade, R. H., 1990, Channel Changes at Cross Sections of the Powder River Between Moorhead and Broadus, Montana, 1975-88, No. 89–407, U.S. Geological Survey.

Pennington, C. H., Baker, J. A., Howell, F. G., & Bond, C. L., 1981, A Study of Cutoff Bendways on the Tombigbee River, E-81-14, U.S. Army Engineer Waterways Experiment Station. https://apps.dtic.mil/sti/pdfs/ADA108896.pdf

Phillips, J. D., Slattery, M. C., and Musselman, Z. A., 2005, Channel adjustments of the lower Trinity River, Texas, downstream of Livingston Dam: Earth Surface Processes and Landforms, v. *30*, p. 1419–1439. doi: 10.1002/esp.1203

Rygel, M. C., and Gibling, M. R., 2006, Natural Geomorphic Variability Recorded in a High-Accommodation Setting: Fluvial Architecture of the Pennsylvanian Joggins Formation of Atlantic Canada: Journal of Sedimentary Research, v. 76, p. 1230–1251. doi: 10.2110/jsr.2006.100

Swanson, K. M., E. Watson, R. Aalto, J. W. Lauer, M. T. Bera, A. Marshall, M. P. Taylor, S. C. Apte, and W. E. Dietrich, 2008, Sediment load and floodplain deposition rates: Comparison of the Fly and Strickland Rivers, Papua New Guinea: Journal of Geophysical Research, v. 113. doi: 10.1029/2006JF000623

Swartz, J. M., Goudge, T. A., and Mohrig, D. C., 2020, Quantifying Coastal Fluvial Morphodynamics Over the Last 100 Years on the Lower Rio Grande, USA and Mexico: Journal of Geophysical Research: Earth Surface, v. 125, doi: 10.1029/2019jf005443

Trampush, S. M., Huzurbazar, S., and McElroy, B., 2014, Empirical assessment of theory for bankfull characteristics of alluvial channels: Water Resources Research, v. 50, p. 9211–9220. doi: 10.1002/2014wr015597

Thorne, C. R., 1991, Bank Erosion and Meander Migration of the Red and Mississippi Rivers, USA: Hydrology for the Water Management of Large River Basins, n. 201, 301–313.

Tye, R. S., 2004, Geomorphology: An approach to determining subsurface reservoir dimensions: AAPG Bulletin, v. 88, p. 1123–1147. doi: https://doi.org/10.1306/02090403100

W.I. van de Lageweg, F. Schuurman, K.M. Cohen, W.M. van Dijk, Y. Shimizu, M.G. Kleinhans, 2015, Preservation of Meandering River Channels in Uniformly Aggrading Channel Belts: Sedimentology, v. 63, n. 3, p. 586–608. doi:10.1111/sed.12229.

Wang, B., & Xu, Y. J., 2018, Dynamics of 30 large channel bars in the Lower Mississippi River in response to river engineering from 1985 to 2015: Geomorphology, v. 300, p. 31–44. doi: https://doi.org/10.1016/j.geomorph.2017.09.041

Wilson, A., Flint, S., Payenberg, T., Tohver, E., and Lanci, L., 2014, Architectural Styles and Sedimentology of the Fluvial Lower Beaufort Group, Karoo Basin, South Africa: Journal of Sedimentary Research, v. 84, p. 326–348. doi: 10.2110/jsr.2014.28

Zhuo, H., Wang, Y., Shi, H., He, M., Chen, W., Li, H., Wang, Y., Yan, W., 2015, Contrasting Fluvial Styles across the Mid-Pleistocene Climate Transition in the Northern Shelf of the South China Sea: Evidence from 3D Seismic Data: Quaternary Science Reviews, v. 129, p. 128–46. doi:10.1016/j.quascirev.2015.10.012.